CERN

Experimental Physics
CERN Summer Student Project Report

Radiation Simulation for the Study of Muon Shield Scenarios in LHCb U2

Jessica Sneddon

Supervisors: Sacha E. R. Medaer,

Gloria Corti

5 September 2025

CERN report

Abstract

LHCb will be increasing its luminosity in Run 5 to a factor of to 10^{34} cm^{-2}s^{-1} and so additional radiation shielding will need to be developed within the detector. This project studied different muon system shielding options for U2, including an additional polyethylene and boron neutron shield behind the HCAL and replacing the HCAL with an iron and concrete block. Simulations were run using FLUKA, a monte-carlo software designed for simulating the interaction and transport of particles, and ratio plots were made in order to compare how the radiative environment changed between each geometry. In addition, the effect of the tungsten and lead bricks recently added within the detector was simulated and analysed. It was concluded that replacing the HCAL with an iron and concrete block increased neutron backscattering within the detector. Furthermore, adding a polyethylene and boron neutron shield mitigated the neutron fluence within the muon system, protecting it from neutron damage.

Contents

1 Introduction

The Large Hadron Collider beauty (LHCb) is an experiment that specialises in CP violation within beauty and charm quark decays. LHCb is built to detect forward particles with the subdetectors placed one behind the other. The detector has been operating since 2010 and is currently anticipating an upgrade known as 'upgrade II', that will be in place for Run 5 and Run 6.

During Run 5 and Run 6 of LHCb (known as HL-LHCb), the luminosity is expected to increase to 10^{34} cm^{-2}s^{-1}, increasing the dose across the detector. The impact of the increased radiation on the electronics can be understood by the type and intensity as it gives a greater understanding of how the electronics are affected by accumulated radiation. These electronics play a large role in the detection and identification of particles and hence, if they degrade, the detector will no longer perform at its maximum efficiency. Radiation simulations provide insight into how increasing the luminosity or changing the material of the detector will change the radiative environment. This allows for well informed decisions to be made about detector and shielding upgrades in the upcoming runs.

2 Theory and Background

2.1 Electromagnetic Calorimeter and the Run 5 Upgrade

LHCb is a forward arm spectrometer composed of multiple sub detectors. The electromagnetic calorimeter (ECAL), located after the VELO and RICH detectors, is a shashlik calorimeter used in the L0 trigger to select events containing b quarks. Furthermore, the ECAL contributes in the reconstruction of neutral particles and particle ID. A shashlik module has alternating layers of scintillator and absorber materials atop each other, perpendicular to the beamline with wavelength shifting (WLS) fibres running between them. The absorber will reduce the energy of a particle travelling through the modules. The energy is converted into light in the scintillator layer, which is carried by the WLS fibres to the photomultiplier tubes (PMTs) [1].

After Run 3, the inner ECAL modules will reach their operational limit of radiation at 40 KGy [2]. In addition, the HL-LHCb runs will have an increased luminosity and hence a higher occupancy in the detector, resulting in overlapping EM showers. In order for the ECAL to maintain its energy resolution and reconstruction efficiency, finer cell granularity is required [2]. The proposed solution to these issues is to use 'spaghetti calorimeters' (SpaCals). SpaCal modules also use scintillator and absorber layers however, the scintillating fibres are inserted into the absorbers. The scintillating fibres then carry the scintillation light to the PMTs [3]. Replacing the shashlik WLS fibres with the SpaCal scintillating fibres increases the light collection efficiency [3].

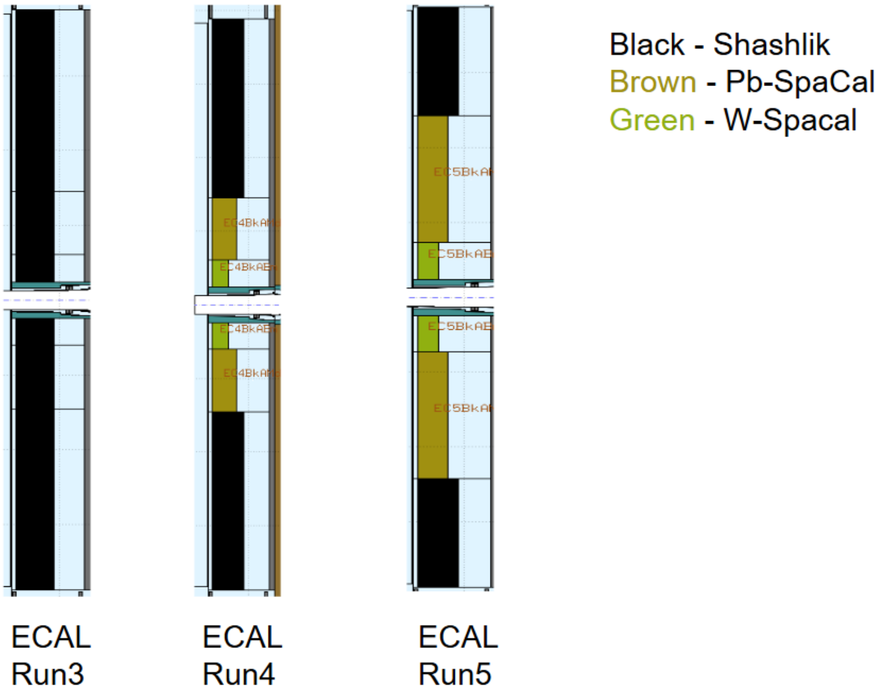

Figure 1: The different ECAL geometries made using FLAIR [4].

Multiple ECAL geometries are being examined with the baseline option combining shashlik and SpaCal modules. Shashlik modules will remain in the outer regions where the dose will be lower relative to the region closest to the beam line. The innermost region will experience > 200 kGy and will require crystal scintillator fibres, tungsten-GAGG crystal modules are a prime candidate [5]. The surrounding intermediate region will be subject to doses ranging from 40 kGy - 200 kGy and will use lead-plastic SpaCal modules, increasing the lead content by 30% [5]. Plastic scintillating fibres are used due to their sensitivity to ionising radiation [6]. The module placement and rhombic like pattern has been determined from a simulation of the expected occupancy at the maximum luminosity (figure 2a). In addition to replacing the inner shashlik modules, the outer modules will be refurbished and the WLS fibres will be upgraded.

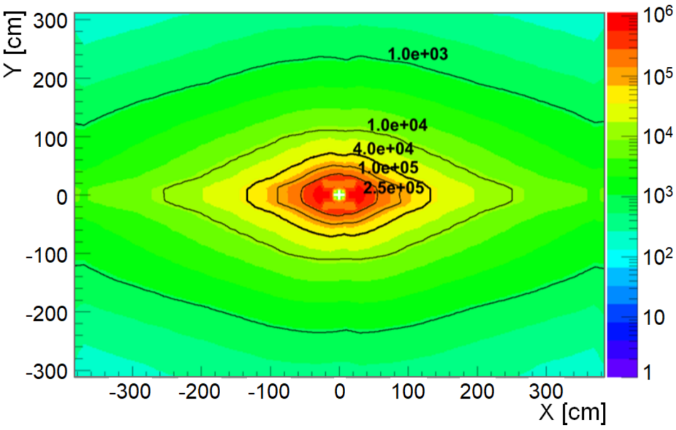

(a) Simulation of expected radiation dose at 300 fb^{-1} of integrated luminosity [2].

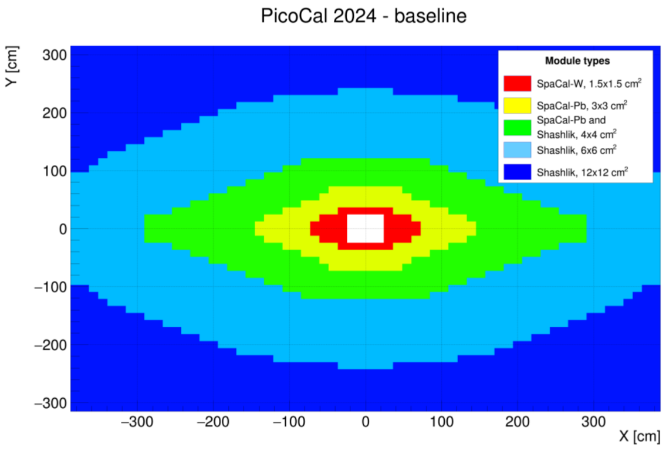

(b) Configuration of ECAL Run 5 [5].

Figure 2: Run 5 ECAL.

2.2 Muon Shielding Upgrade

During the HL-LHCb runs there will be a higher occupancy and dose across the detector. The increased rate in the muon system, specifically M2 and M3, will exceed the capacities of some chambers. To mitigate the rate in the muon system, additional shielding could be added before the system. Multiple options are currently being discussed, including adding additional material (Pb, W, polyethylene) behind the hadronic calorimeter (HCAL) and replacing the HCAL with shielding. The additional shielding would aim to reduce the rate in M2 by a factor of 2 [2].

One possibility is to completely remove the HCAL and reuse the volume for additional shielding, as the HCAL will no longer be used in the trigger from Run 3 [2]. The proposed shielding has a structure that uses an iron core of 1.7 m, an iron/concrete/iron sandwich of 1.7 m with a thickness similar to HCAL and a full concrete part of 1.7 m along the top and bottom as shown in figures 3, 4 and 5. The goal is to increase the amount of material in front of the inner regions where the rate is expected to increase whilst maintaining the same amount of material in the outer regions as the rate will be similar to previous runs.

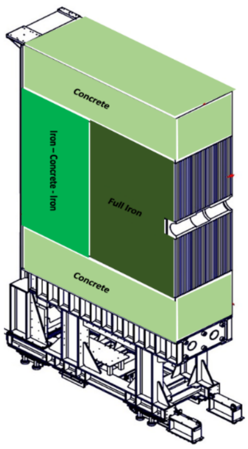

Figure 3: The proposed design of the muon system shielding to replace the HCAL [2].

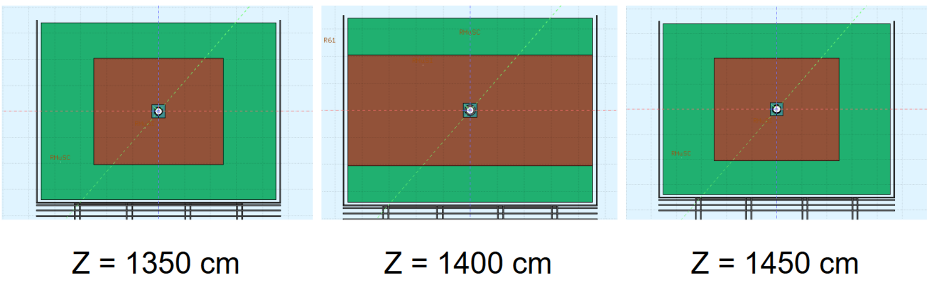

Figure 4: z cross sections of the muon system shielding visualised using FLAIR [4].

Additionally, another neutron shield made of polyethylene and boron has been proposed as a way to reduce the neutron fluence in the muon system. This uses the same material as the current neutron shield in place in front of the calorimeters. It is important to minimise the neutron dose as inelastic collisions of neutrons with the detector material can degrade the electronics and cause permanent damage over time [7].

Shielding needs to be designed in a way that attenuates neutrons in order to increase their interaction probability and absorb them. Light atoms, such as hydrogen (found in polyethylene), are used to attenuate fast neutrons through inelastic collisions [8]. The majority of the neutrons energy is transferred to the proton, slowing the neutrons (thermal neutrons). Boron is then used to absorb these thermal neutrons due to its high neutron capture cross section [8]. This structure is seen within the iron and concrete block as iron mainly attenuates the neutrons and concrete absorbs them.

3 Method

This study examined different combinations of muon system shielding to determine the effect each one has on different estimators. These include neutron fluence, total ionising dose, silicon 1 MeV equivalent neutron fluence and high energy hadron fluence. The combinations were simulated using FLUKA [9], a monte-carlo software that simulates the transport and interaction of particles and is a powerful tool in radiation studies. FLUKA uses custom input files with a unique syntax that defines the geometry and run conditions of the simulation. A limitation during this study was the unknown final geometry for Run 5. Therefore, only changes to the HCAL and ECAL were simulated, however the comparisons made between the different geometries still provide valuable insight into the radiative environment. Ratio plots were made to compare the different combinations and compare the differences between them. Furthermore this highlighted the effect different materials may have on the incoming radiation.

3.1 Scenarios

Five scenarios have been examined within this study. Four of these scenarios include changing the geometry around, and of, the HCAL while the final one removed the recently added lead and tungsten bricks to study the effects these bricks will have. These bricks are currently within LHCb, added during LS2, but their effects have not yet been examined in FLUKA. Lead bricks were implemented just in front of M5 as shielding for the components behind M5 and tungsten bricks were added behind the HCAL as shielding for the muon system.

These scenarios can be seen in figure 5.

- Scenario 1 is the control scenario. It contains the Run 4 ECAL and the HCAL. There are no additions to this scenario and it will serve as the baseline for the Run 4 configuration/geometry. The other scenarios have been compared to this control scenario.

- Scenario 2 includes an additional neutron shield made of boron and polyethylene behind the current HCAL.
- Scenario 3 denotes the scenario in which the HCAL is completely replaced by an iron and concrete block.
- Scenario 4 replaces the HCAL with an iron and concrete block and adds an additional boron and polyethylene neutron shield behind it.

These four scenarios all contain the additional lead and tungsten bricks.

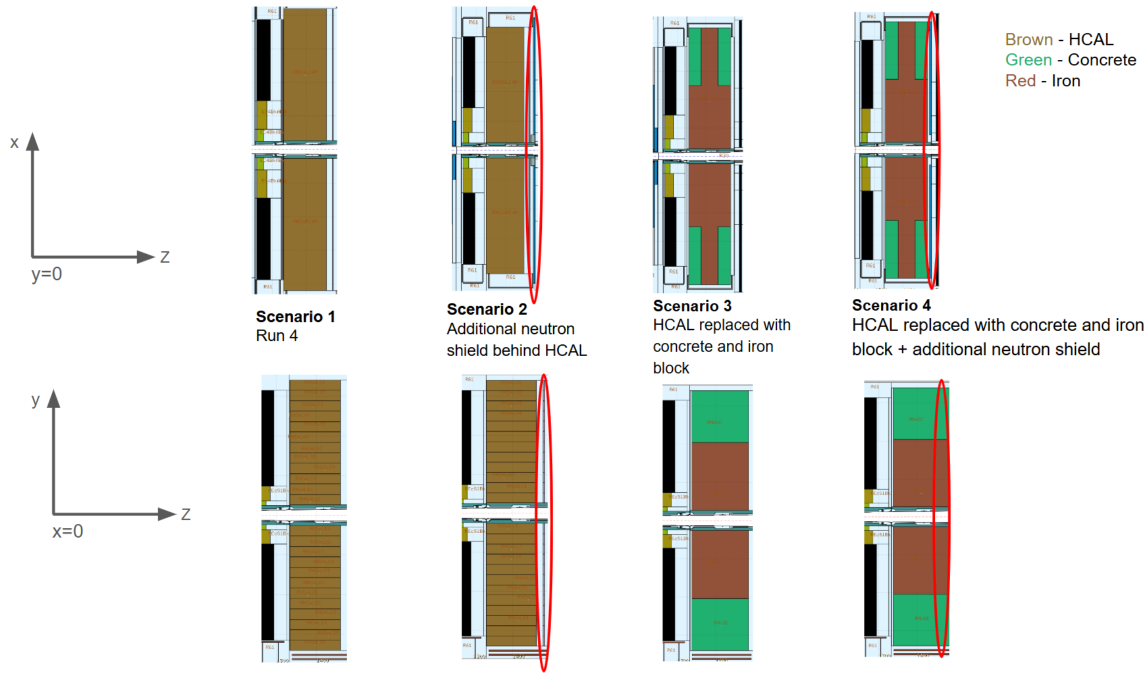

Figure 5: The different combinations of muon system shielding made using FLAIR [4]. The circled parts show the polyethylene and boron neutron shield.

4 Results

The ratio plots were made all use a bin size of 20 cm. Each plot is a slice taken across the x-axis between 0 - 20 cm, placing them at the midpoint in the detector. A map of LHCb is layered atop the plots for clarity.

4.1 Neutron Fluence

Fluence is defined as the time integral of the density flux. In other words, fluence gives the number of particle tracks in a given area. Neutron fluence provides a metric for the amount of neutrons within a specific part of the detector.

4.1.1 Run 4 / Brickless

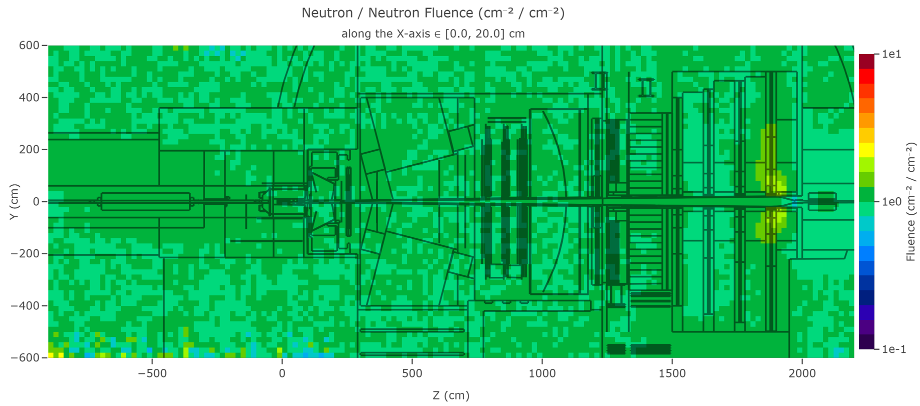

(a) Scenario 1 / Brickless using a log scale.

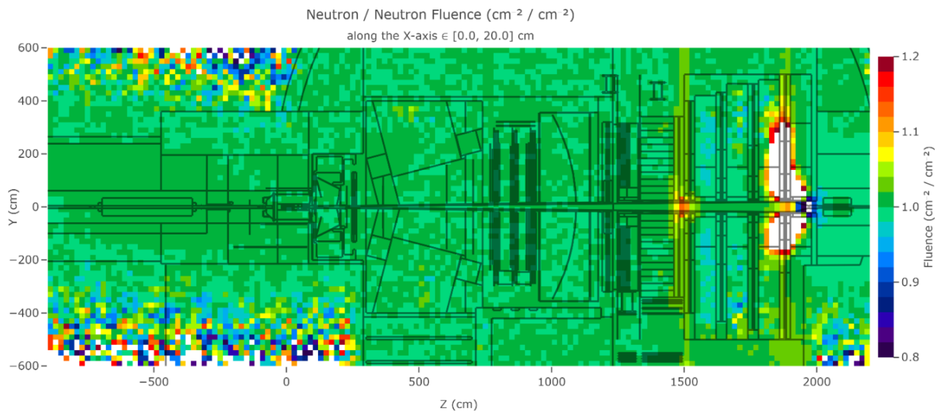

(b) Scenario 1 / Brickless using a linear scale. The white sections correspond to fluences outside of the range.

Figure 6: Plots to show scenario 1 and the brickless scenario neutron fluence using a log and linear scale.

The brickless scenario and scenario 1 compare the detector before and after the bricks were added, Before the lead bricks were added, iron was in their place in the simulation (this is not true of the detector). Figure 6a shows an increase in the neutron fluence surrounding the lead bricks. The maximum increase in fluence within this area is 90% with respect to the brickless scenario. Behind M5, the ratio is < 1 therefore the shielding is functioning. The linear scale seen in figure 6b shows the effect of the tungsten bricks. There is an increase in fluence surrounding these bricks but a decrease in fluence within M2.

4.1.2 Scenarios 2, 3 and 4

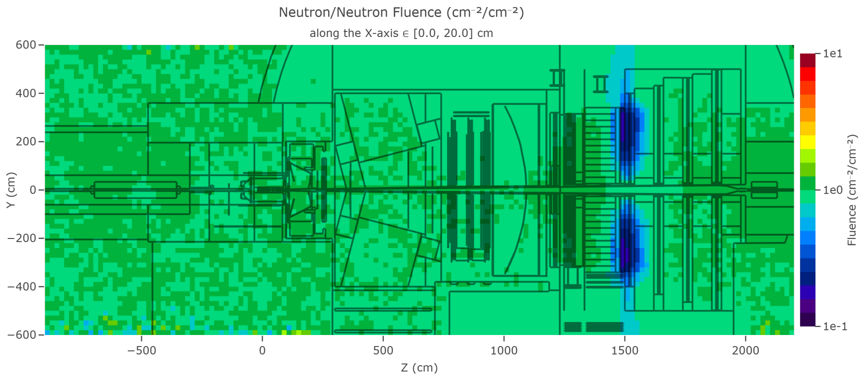

(a) Scenario 2 / Scenario 1

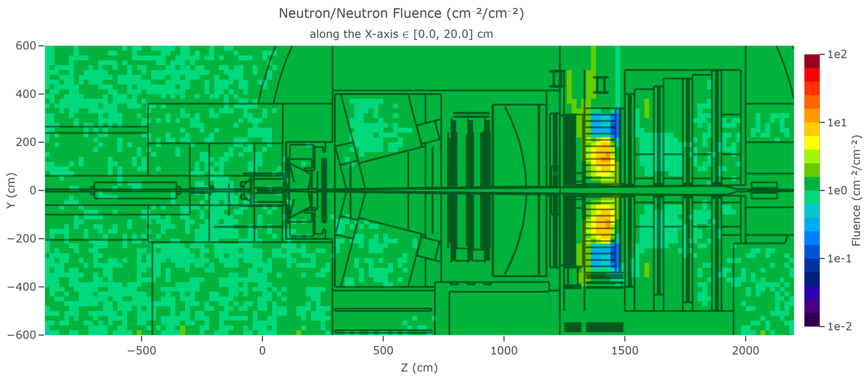

(b) Scenario 3 / Scenario 1

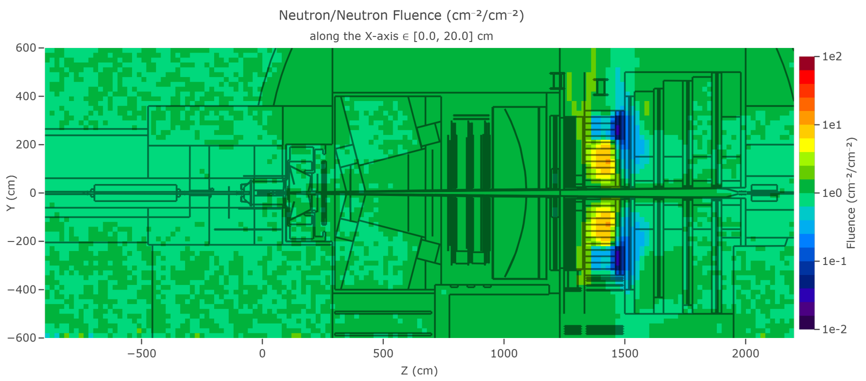

(c) Scenario 4 / Scenario 1

Figure 7: Neutron fluence in LHCb across an x slice [0, 20cm].

When the polyethylene and boron neutron shield was in place, there was a notable reduction of neutron fluence surrounding the shield, and in particular behind the shield where M2 is located as seen in figure 7a. The overall ratio in M2 is < 1, a knock on effect from the neutron shield.

When the HCAL was replaced by the iron and concrete block in figure 7b (scenario 3), the neutron fluence increased across the detector. This increase is most notable within the muon system and around the calorimeters. In M2, the fluence is increased by, at maximum, 80% with respect to Run 4 in scenario 3. This extreme can be seen towards the top of M2. The fluence is mitigated by the additional neutron shield in figure 7c (scenario 4) as the fluence decreased by 70% with respect to Run 4 instead. In addition, there is a significant increase in the backscattering of neutrons from the HCAL area. In both scenarios (with and without the neutron shield) the backscattered fluence is, at most, doubled with respect to Run 4. The iron within the block attenuates and scatters the neutrons through inelastic scattering, explaining why there is a backscattering of neutrons within the detector with the shielding in place.

4.2 Total Ionising Dose

The total ionising dose describes as the amount of energy deposited per unit mass and is useful to understand cumulative damage to materials and electronics.

4.2.1 Run 4 / Brickless

Around the lead bricks, there is an increase in total ionising dose. As lead is denser than iron, it absorbs more high energy radiation such as gamma and x-rays [10] which increased the dose. The linear scale in figure 8b shows a small reduction in dose within M2, a result of tungsten having a high density, making it a suitable shielding for gamma and X-rays [11].

4.2.2 Scenarios 2, 3 and 4

When a neutron shield was introduced (figure 9a), there was a reduced amount of ionising dose as less energy was being deposited in this region. This had a knock on effect in M2 as the ratio is reduced below 1 across the majority of the region.

Figures 9b and 9c display a large dose within the concrete sections of the brick as well as a leakage of dose into the muon system. There is a maximum increase by a factor of 4.4

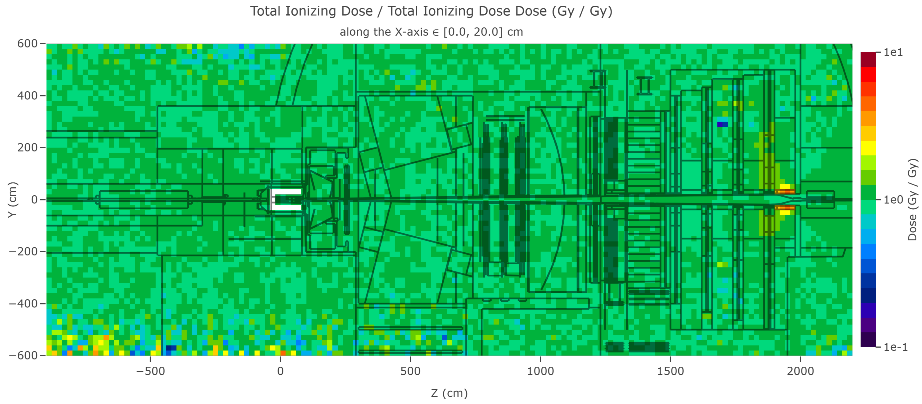

(a) Scenario 1 / Brickless using a log scale.

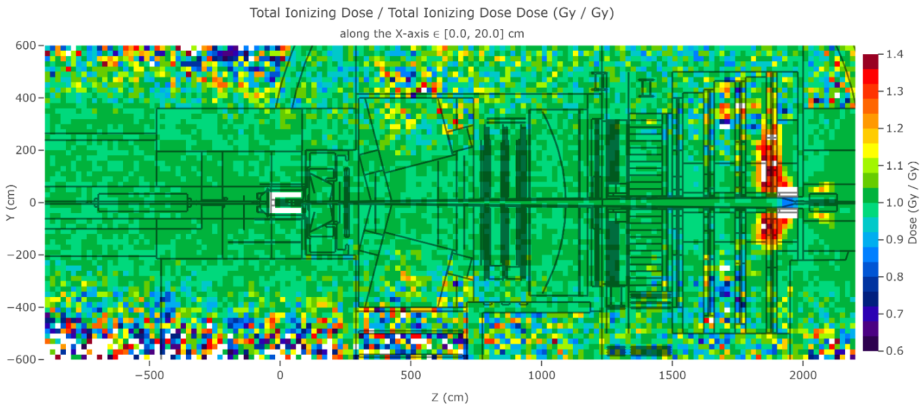

(b) Scenario 1 / Brickless using a linear scale. The white sections correspond to fluences outside of the range.

Figure 8: Plots to show scenario 1 and the brickless scenario total ionising dose using a log and linear scale.

within M2 when there is no neutron shield in place and a maximum increase by a factor of 3 when the neutron shield is added. While concrete is a useful material for absorbing neutrons due to the large number of hydrogen atoms it contains, it is not effective at absorbing other types of radiation. Concrete has, on average, a density of 2.3 g/cm^3, making it an effective attenuator of ionising radiation, resulting in Compton scattering of ionising radiation [12]. This causes the leakage of ionising dose seen within the muon system.

4.3 Silicon 1-MeV Equivalent Neutron Fluence

Silicon 1-MeV equivalent neutron fluence is used to estimate cumulative radiation damage. It is an aggregate of different scorings that are scaled by a coefficient depending on the

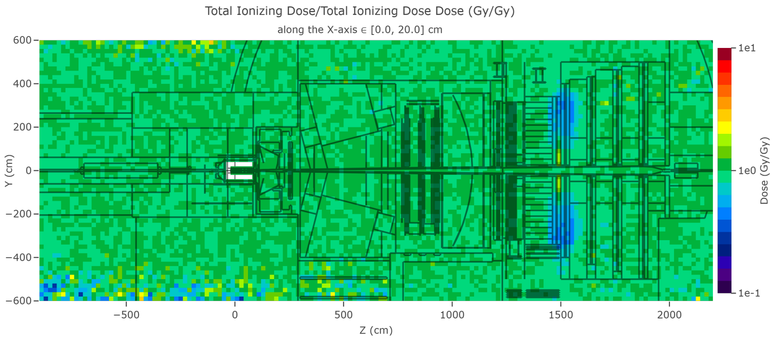

(a) Scenario 2 / Scenario 1

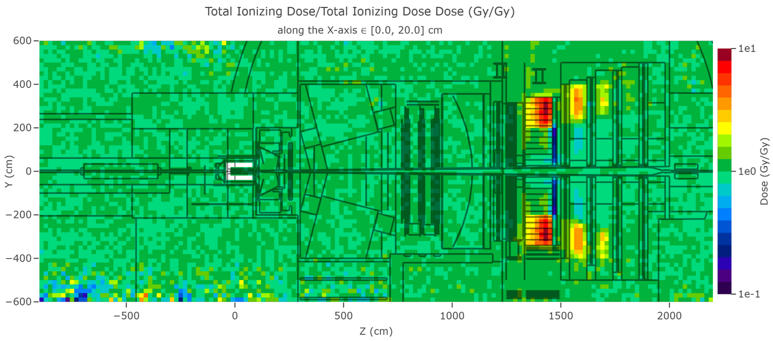

(b) Scenario 3 / Scenario 1

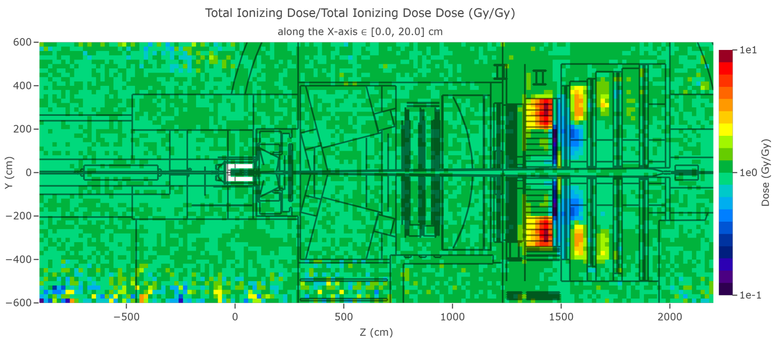

(c) Scenario 4 / Scenario 1

Figure 9: Total Ionising Dose in LHCb across an x slice [0, 20cm].

material considered - in this case, silicon [13]. Silicon is used due to the majority of the electronics being made from silicon.

4.3.1 Run 4 / Brickless

Figure 10a shows a similar pattern to the neutron fluence, with increased fluence surrounding the bricks. The lead bricks are shielding everything behind M5 as the ratio behind M5 < 1 overall when compared to the iron initially in this position. The linear scale shows a reduction in fluence in M2 and a ratio of < 1 across the region as a result of the tungsten bricks.

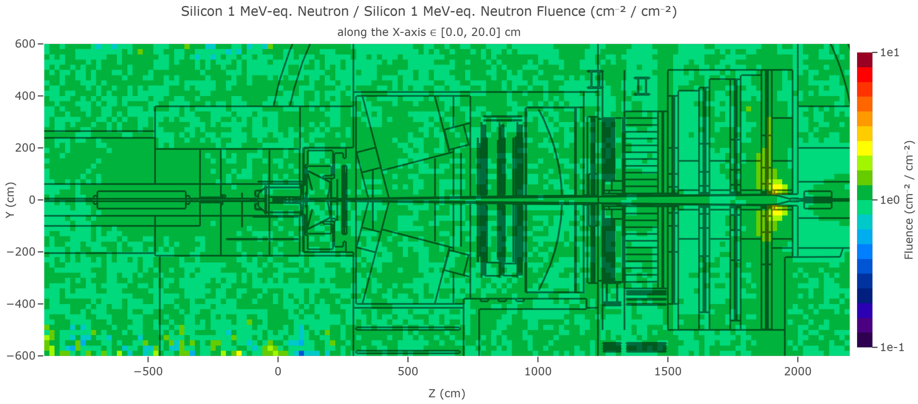

(a) Scenario 1 / Brickless using a log scale.

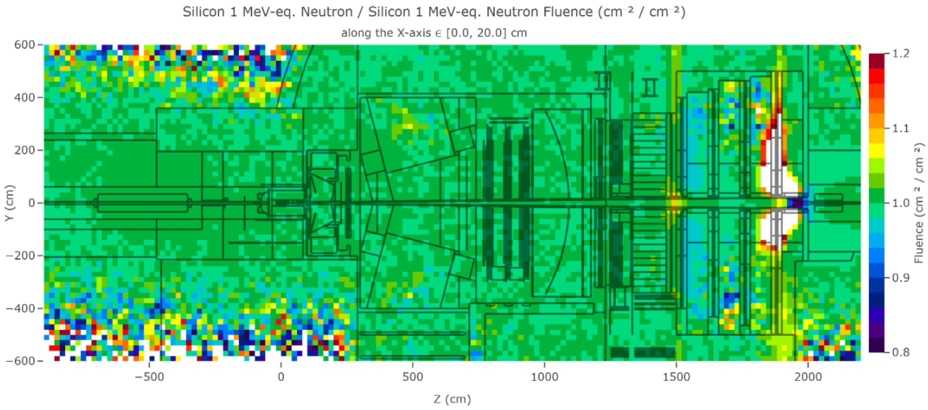

(b) Scenario 1 / Brickless using a linear scale. The white sections correspond to fluences outside of the range.

Figure 10: Plots to show scenario 1 and the brickless scenario silicon 1-MeV equivalent neutron fluence using a log and linear scale.

4.3.2 Scenarios 2, 3 and 4

In figure 11a, there is a reduction of fluence surrounding the neutron shield as expected, resulting in an overall ratio of < 1 within the muon system.

When replacing the HCAL with an iron and concrete block (figure 11b), the iron sections of the block have a larger fluence when compared to Run 4. There is a depletion of fluence within the concrete sections. Along the top of M2, there is a maximum increase of fluence by a factor of 3 when compared to Run 4 however, the ratio is < 1 for a large majority of the muon system. When the additional neutron shield is added (figure 11c), the fluence increases by a factor of 2.8 compared to Run 4, demonstrating that the shield is mitigating the fluence. There is also a reduced fluence in the muon system overall with a ratio < 1. As discussed in section 2.2, neutrons can damage the material through

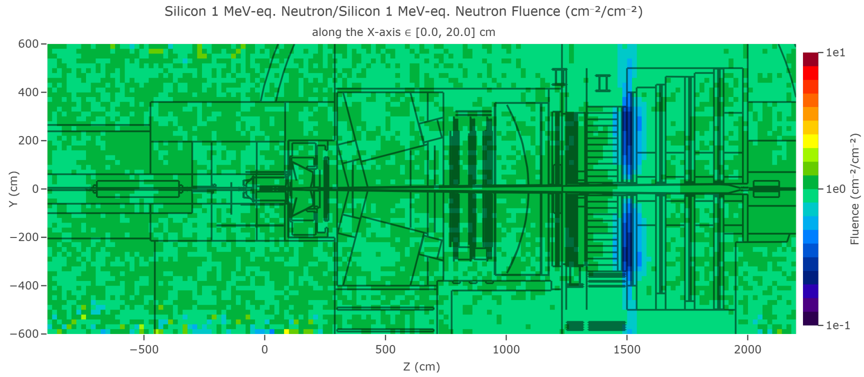

(a) Scenario 2 / Scenario 1

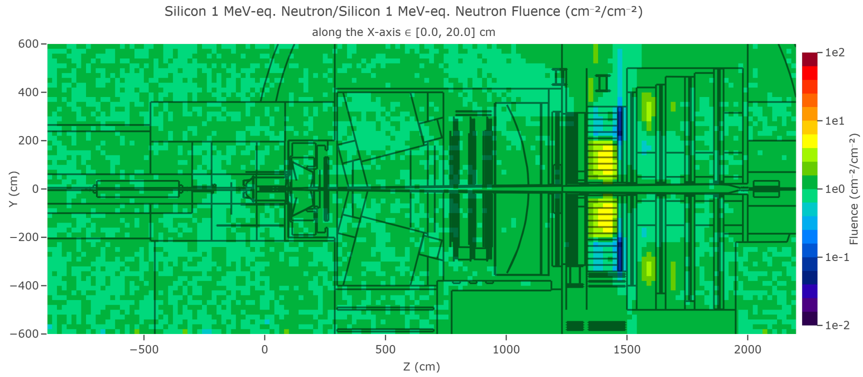

(b) Scenario 3 / Scenario 1

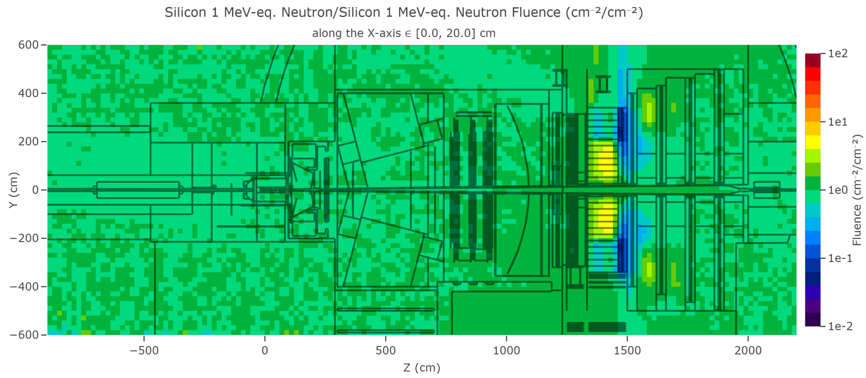

(c) Scenario 4 / Scenario 1

Figure 11: Silicon 1 MeV equivalent neutron fluence in LHCb across an x slice [0, 20cm].

scattering. This leads to an increase in the leakage current within the electronics and reduces the efficiency of the detector [14].

4.4 Hadron (> 20 MeV) Fluence

Hadron (> 20 MeV) fluence describes the high energy hadron fluence which, in this study, refers to any hadron with an energy greater than 20 MeV.

4.4.1 Run 4 / Brickless

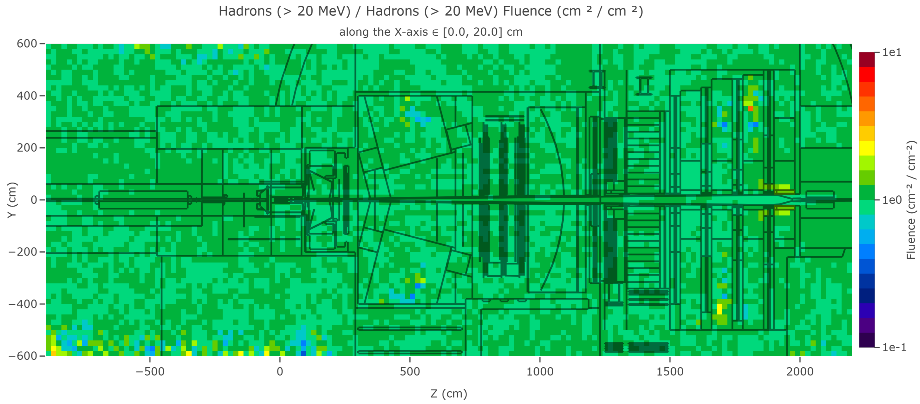

(a) Scenario 1 / Brickless using a log scale.

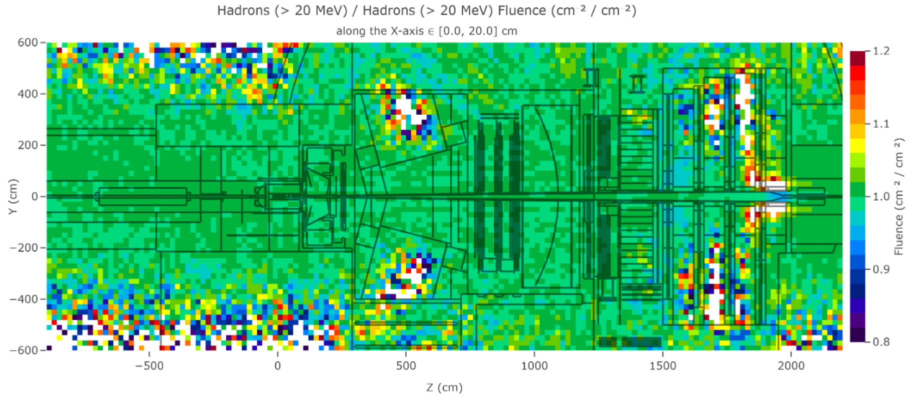

(b) Scenario 1 / Brickless using a linear scale. The white sections correspond to fluences outside of the range.

Figure 12: Plots to show scenario 1 and the brickless scenario hadron (> 20 MeV) fluence using a log and linear scale.

Figure 12a shows that when the lead bricks are in place, there is an increase in the fluence surrounding the bricks. As lead has a higher density than iron [10], it absorbs more hadrons on average than iron does, causing this difference in fluence. The linear scale shows a reduction in fluence surrounding the tungsten bricks and in M2, demonstrating efficient shielding.

4.4.2 Scenarios 2, 3 and 4

Introducing a neutron shield has a small effect on the fluence as there is a slight reduction in the fluence around the shield. In figures 13b and 13c, a similar pattern to the total ionising dose occurs. There is an increased fluence within the concrete sections of the iron

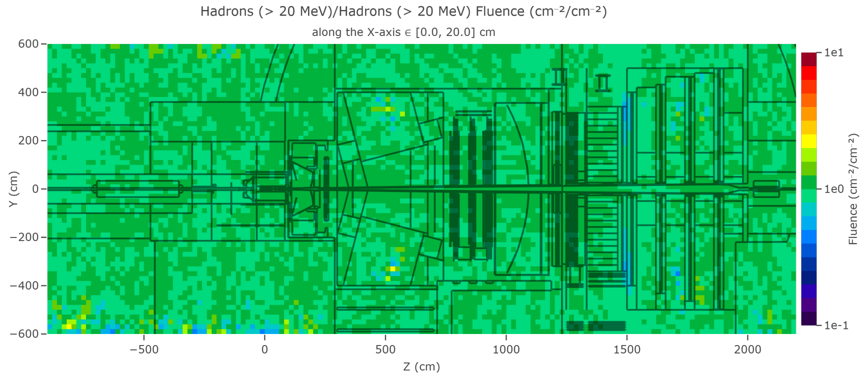

(a) Scenario 2 / Scenario 1

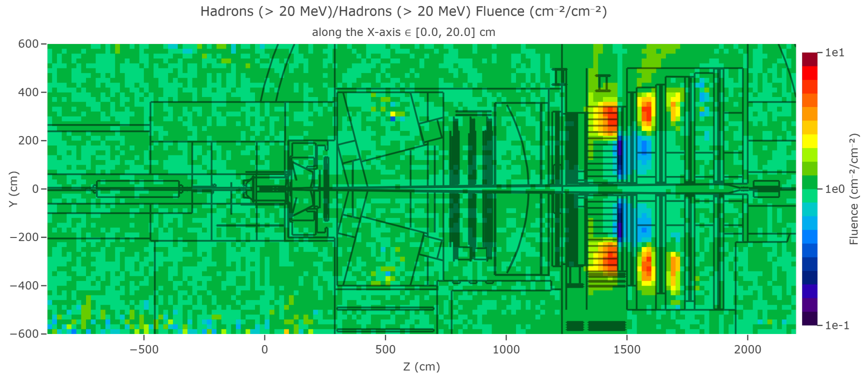

(b) Scenario 3 / Scenario 1

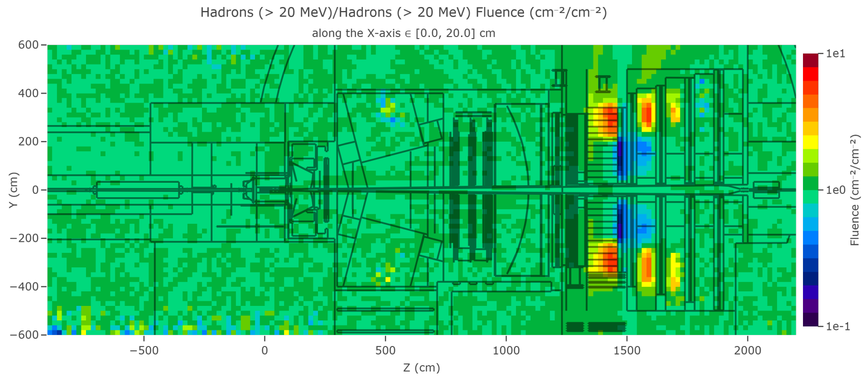

(c) Scenario 4 / Scenario 1

Figure 13: Hadrons (> 20 MeV) fluence in LHCb across an x slice [0, 20cm].

and concrete block causing a leakage into the muon system. The concrete is not absorbing the hadrons, allowing for them to pass through and scatter into the muon system. Iron has a short hadronic interaction length, explaining the depletion of fluence surrounding the iron section of the block [15].

5 Conclusion

In the HL-LHCb runs, additional shielding will need to be added in order to protect the muon system and its electronics from increased radiation. In addition, the ECAL will need to be upgraded as it will reach its operational limit of radiation by the end of Run 3 and it needs to be able to withstand the increased dose.

Introducing an iron and concrete block overall increases the neutron fluence across the detector. The number of backscattered neutrons doubles with respect to Run 4 resulting in an increased fluence within the detector. In addition, the block scatters neutrons into the muon system, increasing the fluence within the system to a greater value than Run 4. The increased neutron fluence within the muon system may have an effect on the electronics and cause them to degrade much faster than previous runs. Adding in a boron and polyethylene neutron shield mitigated the neutron fluence within the muon system. In addition to the block causing an increase in neutron fluence, there is also an increase in total ionising dose and high energy hadron fluence within the muon system. This causes a much larger fluence within these areas and a leakage of these particles into the muon system.

To make a definitive decision on the type of shielding that will be added, further studies will need to be conducted looking at different materials and geometries. To improve this study, the simulations will need to be rerun using the Run 5 ECAL. In addition, comparisons with other monte carlo software is crucial to ensure there are no errors within the simulation.

6 Acknowledgements

I would like the thank my supervisors, Sacha Medaer and Gloria Corti, for offering me this opportunity and supporting me all the way through this project. In addition, I would like to thank the CERN Summer Student team for making this experience possible and a final thank you to the people I met along the way.

References

[1] G I Britvich, A Fenyuk, and V A et al Lishin. A shashlik calorimeter with longitudinal segmentation for a linear collider. 2000.

[2] Framework TDR for the LHCb Upgrade II. Technical report, CERN, Geneva, 2021.

[3] Liupan An, Etiennette Auffray, and Federico et al Betti. Performance of a spaghetti calorimeter prototype with tungsten absorber and garnet crystal fibres. *Nucl. Instrum. Methods Phys. Res., A*, 1045:167629, 2023.

[4] Donadon, André, Hugo, Gabrielle, Theis, Christian, and Vlachoudis, Vasilis. Flair3 – recasting simulation experiences with the advanced interface for fluka and other monte carlo codes. *EPJ Web Conf.*, 302:11005, 2024.

[5] LHCb LHCb collaboration. LHCb Upgrade II Scoping Document. Technical report, CERN, Geneva, 2024.

[6] M.S. Kovačević, S. Savović, A. Djordjevich, J. Bajić, D. Stupar, M. Kovačević, and S. Simić. Measurements of growth and decay of radiation induced attenuation during the irradiation and recovery of plastic optical fibres. *Optics Laser Technology*, 47:148–151, 2013.

[7] Haider F. Abdul Amir and Abdulah Chik. Neutron radiation effects on metal oxide semiconductor (mos) devices. *Nuclear Instruments and Methods in Physics Research Section B: Beam Interactions with Materials and Atoms*, 267(18):3032–3036, 2009. Proceedings of the Ninth International Conference on Computer Simulation of Radiation Effects in Solids.

[8] Kevin Milne. How Borated Polyethylene Works — MarShield Custom Radiation Products — marshield.com. `https://marshield.com/borated-polyethylene-how-it-works/`. [Accessed 01-09-2025].

[9] C. Ahdida, D. Bozzato, and D. et al Calzolari. New capabilities of the fluka multipurpose code. *Frontiers in Physics*, Volume 9 - 2021, 2022.

[10] Your complete guide: Materials that block radiation — radiation detection company — radetco.com. `https://radetco.com/your-complete-guide-materials-that-block-radiation/`. [Accessed 03-09-2025].

[11] A.A. Rotkovich, D.I. Tishkevich, K.A. Mahmoud, M.M. Hanfi, A.A. Bondaruk, S.A. German, T.I. Zubar, M.I. Sayyed, and A.V. Trukhanov. Gamma radiation shielding capacities of the tungsten-sealant composites: Experimental and theoretical study. *Applied Materials Today*, 44:102685, 2025.

[12] Salim Barbhuiya, Bibhuti Bhusan Das, Paul Norman, and Tanvir Qureshi. A comprehensive review of radiation shielding concrete: Properties, design, evaluation, and applications. *Structural Concrete*, 26(2):1809–1855, 2025.

[13] 1-D plot covering CMS tracker, showing FLUKA simulated 1 MeV neutron equivalent in Silicon including contributions from various particle types. 2015.

[14] H.W. Kraner, Z. Li, and K.U. Posnecker. Fast neutron damage in silicon detectors. *Nuclear Instruments and Methods in Physics Research Section A: Accelerators, Spectrometers, Detectors and Associated Equipment*, 279(1):266–271, 1989.

[15] T Cechák, Z Dolezal, and J et al Jakubek. Experimental tests of neutron shielding in the ATLAS forward region. Technical report, CERN, Geneva, 1997.